

Pyrenyl pendent siloxane core dendritic skeletal chain extended multi-walled carbon nanotube reinforced hyperbranched polyimide (MWCNT/PI) nanocomposites

*S. G. Gunasekaran^{1,2}, V. Arivalagan¹, M. Dharmendirakumar²

¹Department of Chemistry, Valliammai Engineering College, Kattankulathur, Kancheepuram 603203, India.

²Department of Applied Science and Technology, Anna University, Chennai-600025, India.

Abstract - A new type of novel polyimide (PI) were structurally designed and developed from pyrenyl pendent diamine and melamine with siloxane-based dianhydride (SDA) in 1-methyl-2-pyrrolidone (NMP) medium via thermal imidization. Varying weight percentages (0.5, 1.0 and 1.5 wt %) of MWCNTs were reinforced with polyimide matrix, followed by thermal curing to obtain MWCNT/polyimide (PI) nanocomposites. The synthesized PI and its nanocomposites were then characterized and confirmed by FT-IR, TGA, DSC, XRD, SEM and TEM analyses. The confinement of segmental motion of the PI chain due to high dispersion uniformity of the MWCNTs and siloxane core caused the increment in the glass transition temperature (T_g) and remarkable elevated thermal stability. Also, the higher T_g of dendritic PI is supported from the chain rigidity of greater extent. The developed polyimide exhibited low dielectric constant (2.1) and low water absorption behaviour (0.48%) due to its silica content. The structural confirmation of PI matrix was afforded by the UV-Vis absorption and strong fluorescent emission bands. The successful incorporation of MWCNT in the PI matrix was evidenced from XRD studies. The SEM studies ascertain the compatibility and smooth morphology MWCNT/PI nanocomposites. The transmission electron microscopy (TEM) studies pointed out that there are no deteriorations in and around the region of MWCNTs, after the formation of nanocomposites.

Key Words: Polyimide, MWCNT, glass transition temperature, thermal stability, dielectric constant, absorbance, fluorescence and morphology

1. INTRODUCTION

Polyimides are the most industrially important thermally stable polymers widely used in applications ranging from microelectronics to aerospace [1-2]. Due to their outstanding properties such as insulating nature, high flexibility, low thermal expansion coefficient, excellent thermal stability and radiation resistance, significant accumulation of electrostatic charge on their surface, high mechanical strength, high modulus and unusual thermooxidative stability, they have been attracted as a significant candidate polymer [3]. Their key drawback is poor solubility and high processing temperature which makes them to process at ambient temperatures. This has been overcome by many chemical modifications such as introduction of flexible linkages [4-6],

bulky units [7-9], bulky pendent substituents [10-11] and noncoplanar moieties [12] in the polymer backbone without dilution of the properties.

Dendritic polymers have a great deal of attention in recent years due to unique properties (i.e., low solution viscosity, high solubility) when compared with their linear analogues [13-17]. Despite dendrimers are perfectly branched and monodisperse molecules, the synthesis involves multistep procedures (protection, coupling and deprotection cycles), leading to high cost and problems in large-scale preparation. To replace dendrimers for most cases, hyperbranched polymers are widely used to have similar properties as well-defined architectures as dendrimers. Their ease of preparation the hyperbranched polymers are of more significance than dendrimers from the viewpoint of industrial applications. Till to date many hyperbranched polymers have been synthesized such as polyphenylene, poly(ether ketone), poly [4-(chloromethyl) styrene], m-polyaniline, polycarbonate, polyesters, aromatic polyamides, etc. [18]. Recent researches show remarkable increase in the area hyperbranched aromatic polyimides (HBPIs) [19-20].

Over the past decade, great strides have been made in exploiting the unique combination of electronic and mechanical properties of carbon nanotubes (CNT) [21]. CNT/polymer composites are promising materials whose mechanical properties and electrical conductivity can be enhanced by the addition of CNT [22-23]. Consequently, the CNT/PI nanocomposites thus obtained will be of a greatly superior quality, and homogeneity. Several researchers have demonstrated the benefits of the formation of CNT incorporated PI nanocomposites successfully [24].

In recent years, polyimide nanocomposites have been developed by incorporating the functionalized multi-walled CNTs (MWCNTs) by Qu et al [25] and Yuen et al [26] with excellent mechanical properties. Ausman and co-researchers [27] introduced the chemical functionalization of CNT by a strong mixed-acid treatment to increase the interfacial interactions between the PI matrix and CNT, which would be favorable for the homogeneous dispersion of CNTs in a polymer matrix [28].

Siloxane based organic-inorganic hybrid nanocomposites are of great concern because of their unique properties, such as thermal stability, flexibility, hydrophobicity, low dielectric

constant, significant gas permeability, and good film-forming ability and numerous potential applications [29-30]. Silicone resins containing the linear Si-O-Si structural units are easy to decompose through inter-chain rearrangements, leading to the formation of a passive layer, and hence, improved thermal resistance and flame retardancy [31]. Li and his co-workers incorporated the rigid nadic anhydride based imide segment into the epoxy, with the improvement of its flexibility and toughness [32]. Chen et al reported the formation of a network structure by the inclusion of a siloxane segment into benzoxazine. The thermal stability was noticeably increased due to nadic anhydride on the chemical structure of the siloxane unit [33]. New types of siloxane core-modified organosoluble novel polyimide/multi-walled carbon nanotube nanocomposites were prepared and their properties were studied by Gunasekaran and his team [34-35]. Nanosized silica reinforced heteroaromatic rings containing pyridine based polybenzoxazine were also synthesized and reported [36].

In the present work, a novel hyperbranched dendritic polyimide containing siloxane core pyrene pendant has been structurally designed and synthesized. The present study describes the preparation of MWCNT reinforced siloxane modified dianhydride based polyimides. Thus, the developed nanocomposites are expected to possess better thermal, morphologies and electrical properties required for high performance applications in aerospace and microelectronics. For achieving this, in-situ polymerization followed by subsequent imidization to get MWCNT-PIs. The nanocomposites were characterized by described by FT-IR, DSC, TGA, dielectrical, UV-vis, PL, SEM and TEM analyses.

2. EXPERIMENTAL METHODS

The MWCNT fillers were procured from the Applied Science and Innovation Pvt. Ltd, Pune, India. The specifications of the MWCNT were: diameter - 20-45 nm, length - 1.0-40 μm , and surface area - 40-500 m^2/g . The MWCNTs were purified according to the reported procedure [37]. 5 - norbornene - 2, 3 - dicarboxylic anhydride (Nadic anhydride) and 1, 1' 3, 3'-tetramethyl disiloxane were purchased from Acros organics Ltd and Alfa-aesar, India. The monomers such as siloxane core dianhydride (SDA) and 4-(1-Pyrene)-2,6-bis (4-aminophenyl) pyridine (PBAPP) were synthesized as per the reported procedure. N-methyl-2-pyrrolidone (NMP), N, N-dimethyl formamide (DMF), Tetrahydrofuran (THF) H_2SO_4 , HNO_3 and Melamine were purchased from SRL, India.

2.1 Materials

The MWCNT fillers were procured from the Applied Science and Innovation Pvt. Ltd, Pune, India. The specifications of the MWCNT were: diameter - 20-45 nm, length - 1.0-40 μm , and surface area - 40-500 m^2/g . The MWCNTs were purified according to the reported procedure [37]. 5 - norbornene - 2, 3 - dicarboxylic anhydride (Nadic anhydride) and 1, 1' 3, 3'-tetramethyl disiloxane were purchased from Acros organics Ltd and Alfa-aesar, India. The monomers such as siloxane core dianhydride (SDA) and 4-(1-

Pyrene)-2,6-bis (4-aminophenyl) pyridine (PBAPP) were synthesized as per the reported procedure. N-methyl-2-pyrrolidone (NMP), N, N-dimethyl formamide (DMF), Tetrahydrofuran (THF) H_2SO_4 , HNO_3 and Melamine were purchased from SRL, India.

2.2 Synthesis of Siloxane core modified Anhydride (SDA)

The siloxane core dianhydride moiety [(5, 5'-(1, 1, 3, 3 - tetramethyl - 1, 1, 3, 3-disiloaxanedialyl) bisnorbornene - 2, 3 - dicarboxylic anhydride] was synthesized, using nadic anhydride and 1, 1' 3, 3'- tetramethyl disiloxane (Scheme 1) as per the method reported in literature [33, 38].

$^1\text{H-NMR}$ spectral data (ppm, 500 MHz, $\text{d}_6\text{-CDCl}_3$) shows δ : 0.03-0.05 (m, 12H), 0.62-0.67 (m, 2H), 1.54-1.69 (m, 8H), 2.76-2.80 (m, 2H), 2.9-3.1 (m, 2H), 3.39-3.42 (m, 4H).

2.3 Synthesis of PBAPP

Pendant pyrene-pyridine core aromatic diamine (PBAPP) monomer was prepared according to reported procedure [39-43]. The synthesized monomer was then characterized and confirmed by $^1\text{H-NMR}$, and FT-IR techniques and matched with earlier reported data.

Spectral data

FT-IR spectral data of PBAPP (KBr): 3376, 1615, 1471 cm^{-1} .

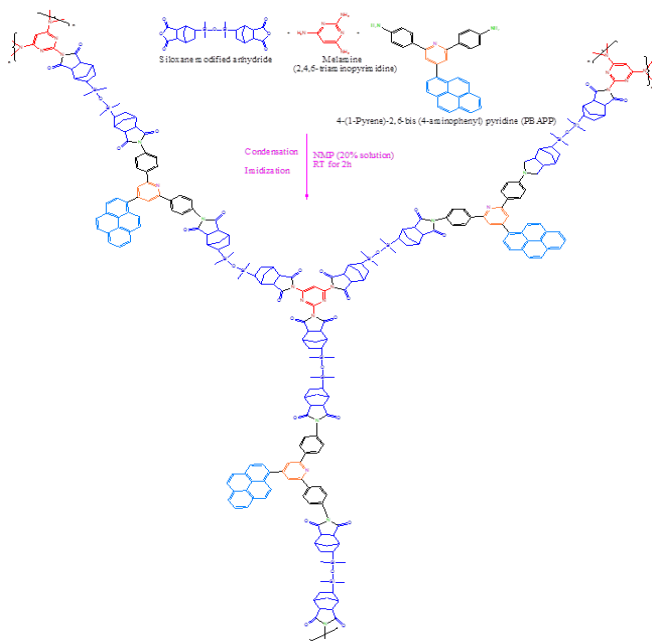
$^1\text{H-NMR}$ spectral data PBAPP (ppm, 500 MHz, DMSO-d_6) shows δ : 8.77-8.60 (d, 1H), 8.55-8.51 (d, 1H), 8.50-8.40 (d, 1H), 8.34 (s, 2H), 8.32-8.27 (m, 3H), 8.07-8.00 (t, 1H), 7.97-7.86 (d, 4H), 7.45 (s, 2H), 6.82-6.80 (d, 4H), 5.43 (s, 4H).

2.4 Preparation of Amine functionalized Carbon Nanotubes (α -MWCNT)

1.0 g of MWCNTs was debundled in 80 ml of concentrated H_2SO_4 and HNO_3 with a volume ratio of 3:1 using an ultrasonicator for 10 min. The mixture was stirred at 60°C for 24 h and then separated by centrifugation, washed several times with deionized water and dried in a vacuum at 70°C for 24 h to get acid-functionalized MWCNTs (α -MWCNT) [44].

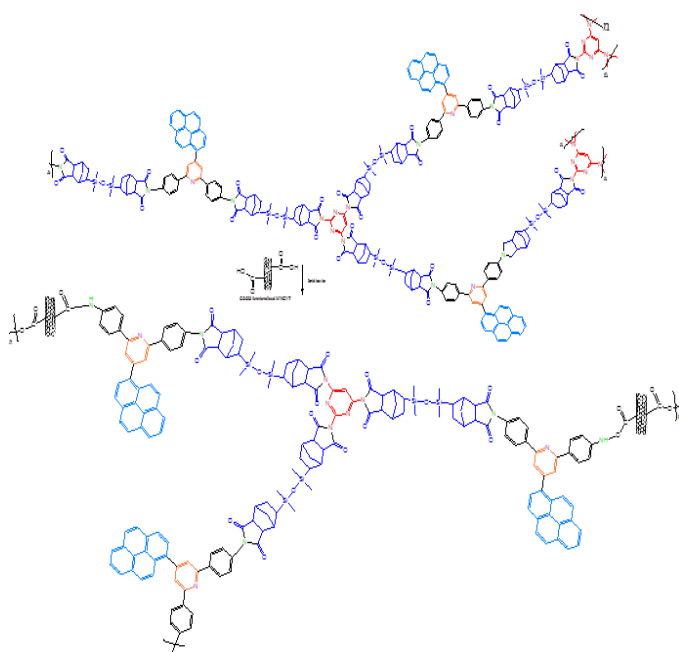
2.5 Preparation of MWCNT reinforced Polyimide (PI) Nanocomposites

The structurally modified neat polyimide was prepared via condensation of 4-(1-Pyrene)-2, 6-bis (4-aminophenyl) pyridine (PBAPP), melamine with siloxane core modified dianhydride (SDA) using NMP as a solvent [16, 38]. The mole ratio of SDA, Melamine and PBAPP was 1:3:1. First, PBAPP was dissolved in NMP and then siloxane core modified dianhydride (SDA) was added to the diamine/melamine solution to make slurry with 20 % (w/v) solid content followed by stirring at RT for 6 h. Then, PAA was poured onto silane coated glass plate.



Scheme 1. Schematic representation of the synthesis of polyimide

The plates were dried for 10 h at 40 °C, and then heated to 100 °C for 1 h in an air circulation oven followed by keeping another 1 h at 150, 200, and 250 °C, respectively and finally, heated to 300°C for 30 min to complete the imidization reaction (Scheme 1).



Scheme 2. Schematic representation of the preparation of MWCNT/PI nanocomposites

For the preparation of the MWCNT incorporated polyimide (MWCNT/PI) nanocomposites, the MWCNTs were dispersed and added to PAA solutions prepared above to form a series of MWCNT/PAA suspensions with MWCNT concentrations of 0.5, 1.0 & 1.5 wt % vs. PAA solid contents [51]. The suspension was sonicated for 1 h at room

temperature, followed by vigorous stirring for another 2 h at RT. The obtained solutions were cast and imidized according to the procedure reported above to get MWCNT incorporated PI nanocomposites (Scheme 2).

2. CHARACTERIZATION

3.1 Physico-Chemical Studies

FT-IR spectra were recorded on a Perkin Elmer 6X FT-IR spectrometer. About 100 mg of optical-grade KBr was ground with sufficient quantity of the solid sample to make 1.0 wt % mixture for making KBr pellets. After the sample was loaded, a minimum of 16 scans were collected for each sample at a resolution of ± 4 cm⁻¹. All 1H NMR analyses were done in d-CHCl₃ recorded on a Bruker 300 spectrometer.

3.2 Thermal Studies

A Netzsch DSC-200 differential scanning calorimeter was used for the calorimetric analysis. The instrument was calibrated with Indium supplied by Netzsch. Measurements were performed under a continuous flow of nitrogen (60 mL/min). All the samples (about 10 mg in weight) were heated from ambient to 400 °C and the thermograms were recorded at a heating rate of 10 °C/min. Thermogravimetric analysis (TGA) was performed in a DSC-2920 from TA Instruments coupled with a TA-2000 control system. The samples were heated at a scanning rate of 10 °C/min under nitrogen atmosphere in order to diminish oxidation.

3.3 Dielectric Constant

The dielectric constants of the neat PIs and the MWCNT/PI nanocomposites were determined with the help of an impedance analyzer (Solartron impedance/gain phase analyzer 1260) using a platinum (Pt) electrode at 30°C in a frequency range of 1 MHz.

3.4 UV-Vis Absorption and Emission Properties

The neat PIs and MWCNT/PI nanocomposites were characterized by UV-vis-NIR spectrophotometer (UV-vis-NIR) (U-4100, Hitachi, Japan). The absorbance of the solution was measured with a wavelength range of 200 to 1300 nm. The emission properties of the MWCNT/polyimide nanocomposites were studied using Fluorescence spectrophotometer (Cary Eclipse, FL1201M002, Japan) with wavelength range from 400 to 800 nm.

3.5 Water Absorption Behaviour

The MWCNT/PI specimens were tested for water absorption properties as per ASTM D 570. The cured specimens (dimensions: 100 mm square, 3 mm thickness) were immersed in distilled water for 48h. They were then removed from water, and weighed to an accuracy of 0.0001g.

3.6 Morphological Studies

Scanning electron microscope (SEM) (Hitachi S-3400N) was used to observe the SEM morphology of the fractured surfaces of the MWCNT/PI nanocomposites. The Transmission electron microscope (TEM) observations were performed on a JEOL JEM-3010, with an accelerating voltage of 300 KV. The samples were prepared by dipping a copper TEM grid into the MWCNT dispersion and then subsequent drying.

4. RESULTS AND DISCUSSION

4.1 Synthesis of Diamine Monomers

The structures of compounds PBAPP were confirmed by FT-IR and NMR spectroscopic analysis [34, 40]. The ¹H NMR (500 MHz) spectrum of PI showed no amide and acid protons, confirming full imidization. Also, all protons in the backbone of the pyrene based pyridine core diamines can be assigned, as shown in Figure 1. A signal appeared at 5.42 and 5.76 ppm due to the amino groups in the ¹H NMR spectrum of PBAPP clearly confirms that the diamine (PBAPP) prepared herein is consistent with the proposed structure.

The compound PBAPP gave a characteristic band at 3376 cm⁻¹ which indicated the symmetric stretching of the amino group. The characteristic absorptions of the C=N group appeared at 1471, and the characteristic band of the amino group N-H bending at 1620 was appeared. In addition, the C-O-C stretching vibration was shown at wavelength of 1244 cm⁻¹ for PBAPP. The C=C aromatic stretching was observed at 1504 cm⁻¹.

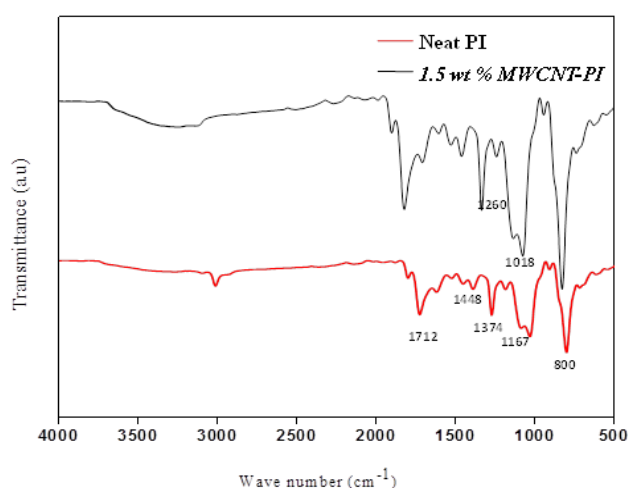


Figure 1. FT-IR spectra of neat PI and MWCNT-PI nanocomposites

4.2 Synthesis of MWCNT reinforced Polyimide (PI) Nanocomposites

MWCNT/PI nanocomposites were synthesized by solution casting and thermal imidization methods. The formation of the neat PI and MWCNT/PI nanocomposites was

been confirmed by FT-IR spectra. Figure 1 shows the FT-IR spectra of neat PI and MWCNT/PI nanocomposites with different wt % of MWCNTs. The FT-IR spectra of siloxane-modified neat PIs showed characteristic bands, at around 1260 cm⁻¹ corresponding to the stretching of -Si-CH₃ respectively. The strong absorption bands appeared at 1712 cm⁻¹ (symmetric C=O in the imide groups) and 1374 cm⁻¹ (-C-N in the imide groups) after thermal imidization. At 1447 cm⁻¹, there is a CH₃ antisymmetrical deformation. The peak at 1167 cm⁻¹ was resulted from the CH₂ wagging of imide rings. The absence of OH bands at 3530 and 3400 cm⁻¹ confirms the imidization of poly (amicacid) group present in the condensation reaction [32].

Table 1. Thermal and dielectric properties of neat PI and MWCNT-PI nanocomposites

Compositi on	Tg (°C)	T10 (°C)	T20 (°C)	Char yield (700°C)	Dielect ric consta nt @	LOI
					298 K (ε') 1MHz	
Neat PI	192	375	420	48.0	4.0	36.7
0.5 wt % MWCNT-PI	193	380	435	50.5	4.8	37.7
1.0 wt % MWCNT-PI	198	390	455	55.0	5.1	39.7
1.5 wt % MWCNT-PI	207	415	499	66.8	5.3	44.2

After the incorporation of MWCNT to the PI matrix, the carboxyl group of MWCNT reacts with the diamine of PI and is confirmed by peak appearing at 1018 cm⁻¹ corresponding to the Si-O-Si linkage stretching and disappearance of peak at 1550 and 1660 cm⁻¹ corresponding to the amide groups. These absorption peaks confirmed that siloxane dianhydride was imidized into polyimide with incorporation of MWCNTs and match well with the earlier reported data [28, 37].

4.3 Thermal Properties of MWCNT/PI Nanocomposites

4.3.1 Thermogravimetric Analysis

The thermal stability of the cured neat PI and MWCNT/PI nanocomposites was ascertained by thermogravimetric analysis. The thermal stability of these neat PI and MWCNT/PI was compared based on the temperature of 10 and 20 % decomposition. As shown in Table 1, the initial decomposition temperature of the resulting PI was in the range of 320-370 °C and the temperatures at 10 and 20 % weight loss of PI were in the range of 375 and 420 °C respectively. From Figures 2, it was indicated that the initial degradation temperatures for the neat PI system were lower than those of MWCNT incorporated PI systems reported in the present work [35].

The incorporation of siloxane core modified dianhydride and dendritic skeleton may alter the thermal behaviour of

polyimides. However, after polymerization, the thermal stability has been significantly increased due to the combination of the presence of thermally stable imide rings and Si-O-Si linkages in the polymer backbone [45]. Moreover, while using this type of end-capped siloxane containing dianhydride, it could be very difficult to undo the Si-O-Si linkage from the anhydride monomer, which would contribute to enhance the flame retardant properties of the prepared polyimides [46-47].

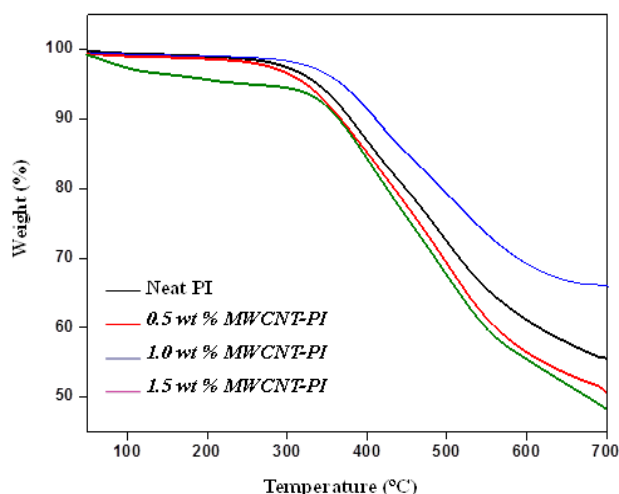


Figure 2. TGA thermograms of neat PI and MWCNT-PI nanocomposites

Moreover, the presence of rigid pyridine moiety along pyrene group with flexible linkage in its structure, increase thermal stability comparatively high. In case of neat PI having flexible phenoxy linkages possess less thermal stability compared to neat PI system. Hence, the cured PI obtained from these polymer precursors are expected to be less brittle than those of the ordinary PI because larger polymer segments would be available for internal motion. The char yield of the neat PI was 48.0 %, when heated to 700 °C in nitrogen, confirming that this polymer have good thermal stability and self-extinguishing property [48-49].

However, the thermal stability of the MWCNT/PI nanocomposites was increased to about 40 °C by incorporating 1.5 wt % of MWCNT content as clearly seen from TGA curves (Table 1). The improvement in thermal stability is due to the reinforcement and good interfacial interaction of acid functionalized MWCNTs with the PI matrix and which may limit the continuous decomposition of the PI phase [26, 34].

4.3.2 Differential Scanning Calorimetry

Glass transition temperature (T_g) of the neat PI and MWCNT incorporated nanocomposites was determined by DSC measurements and listed out in Table 1. It can be seen that, compared with neat PI (T_g = PI: 192 °C), the T_g was increased by about 15°C by incorporating only 1.5 wt % MWCNTs into the PI system (Figure 3). PI containing amino

phenyl moiety (PI) have higher T_g due to the increased rigidity of the polymeric chain in the former.

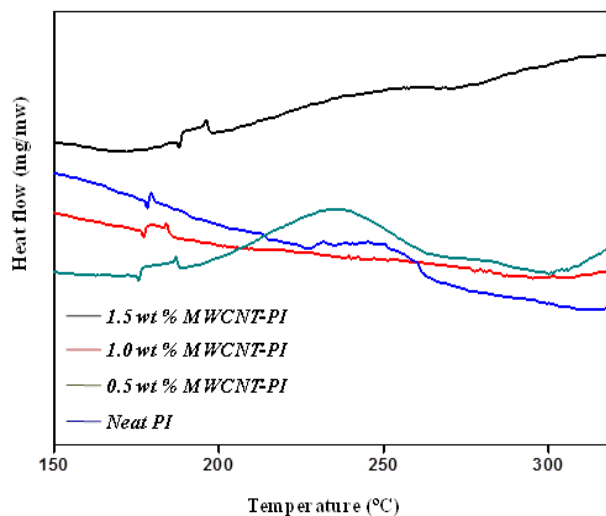


Figure 3. DSC thermograms of neat PI and MWCNT-PI nanocomposites

In case of neat PI system, the diamine moiety was PBAPP and in which, the segmental motions of the polymer chain were restricted as there is no flexible linkages. The end phenyl ring present in the diamine moiety tilts easily at any angle, because of the flexible ether linkages, since there is no hindering group in it (rotational freedom) in the case of neat PI. Thus, due to this size effect, the homogeneous rigidity resulting from this type of flexibility led to a decrease in the glass transition temperature of the neat PIs [50].

The values of T_g were increased with an increase in the MWCNT content. The increased glass transition temperature of the MWCNT/PI nanocomposites may also be explained by the constraint effect of MWCNTs due to the significant nanoreinforcement effect and the augmentation of cross-link density, which could restrict the motion of molecular chains, and hence, significantly increased the glass transition temperature of the MWCNT/PI nanocomposites increased with acid modified MWCNT content [44, 51].

4.3.3 Limiting Oxygen Index

The non-flammability of the neat PBI and MWCNT reinforced PI nanocomposites is explained from the value of limiting oxygen index (LOI). From Figure 4, it was shown that LOI of neat PI [53] was 36.7 % whereas MWCNT-PI showed 37.7-44.2 % (Table 1). The LOI value of MWCNT incorporated PI nanocomposite is higher than that of the neat PI matrix with increasing weight % of MWCNT. This elevated flame retardancy was due to the presence of siloxane unit as well as the nanoreinforcement effect of MWCNTs in the nanocomposites. The significant increase in the value of LOI indicates that the MWCNT reinforced PI nanocomposites exhibit better flame retardancy [47].

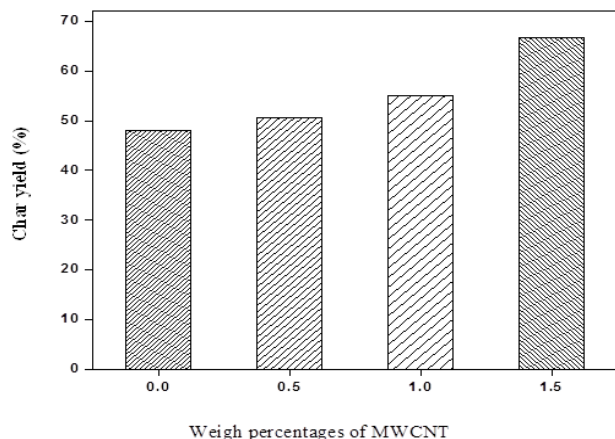


Figure 4. LOI values of neat PI and MWCNT-PI nanocomposites

4.4 Dielectric Properties

The dielectric constants (ϵ') of the neat PBZs and MWCNT-PBZ hybrid nanocomposites were measured, by using the impedance analyzer in the frequency range of 1 MHz at RT (Figure 5). Dielectric constant data of the neat PI and MWCNT incorporated PI nanocomposites are presented in Table 1.

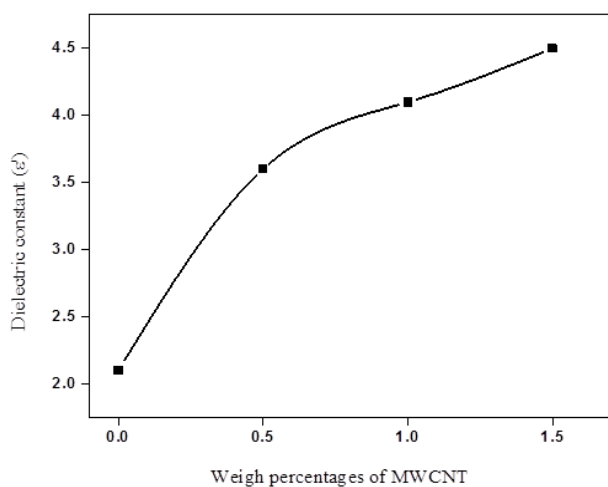


Figure 5. Dielectric behaviour of neat PI and MWCNT-PI nanocomposites

The data obtained from the dielectric studies indicate, that the siloxane core modified PI lowered significantly with the incorporation of less polarizable components. This is because the introduction of a siloxane moiety and a phenylene ether unit into the diamine part induces the dilution effect of the polar imide ring and reduces the values of the dielectric constant of neat PI [50-51].

Furthermore, as the concentration of the MWCNT increased, the free volume and relative chain rigidity decreased. As a result of this, the values of the dielectric constant of the resulting MWCNT-PBZ nanocomposites were

increased (4.8-5.9 at 1MHz) [47, 51-52]. This is due to the high electrical conductivity and current-carrying capacity of MWCNT which enhances the dipole-dipole interactions. Hence, the development of these MWCNT/PI nanocomposites would play a part in the development of the effective and efficient functioning of electronic instruments.

4.5 Water Absorption Behaviour

The water absorption behaviour of the neat PI and MWCNT-PI nanocomposites was studied and data is plotted as shown in Figure 6. It was observed that the neat PI exhibited low water absorption behaviour than that of the MWCNT/PI nanocomposites (Table 1). This is due to the insertion of siloxane core dianhydride into the PI backbone, resulted from low polarity as well as the hydrophobic nature of the siloxane core moiety present in the PI system [30, 53].

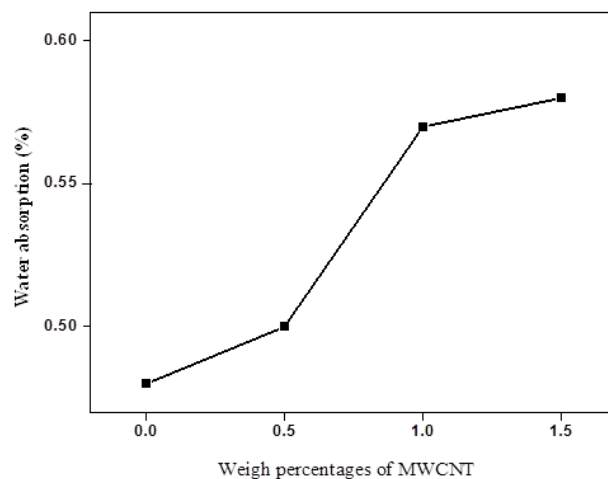


Figure 6. Water absorption behaviour of neat PI and MWCNT-PI nanocomposites

The water absorptions of neat PIs and 1.5 wt % MWCNT/PI nanocomposites were 0.48 % and 0.58 % respectively as can be seen from Figure 6. This increment may be attributed to the acid groups present in the surface of the MWCNTs; further addition in the concentration of the MWCNTs increased their water absorption properties.

4.6 Optical Properties

4.6.1 UV-Vis Absorption Spectra

The UV-vis absorption studies of the neat PI and MWCNT/Pis were investigated in THF using UV-Vis radiation as shown in Figure 7. It was seen that neat PI display one prominent band with an unsymmetrical shape and an adjoining shoulder. The neat PI shows a strong absorption at 281 nm which is blue shifted by about 10 nm from that of diamine after polycondensation ($n-\pi^*$ transition). In addition, the most bathochromically shifted transitions bands in the region of 300- 400 nm is mainly assigned to that arising from pyrene-based $\pi-\pi^*$ transitions [48].

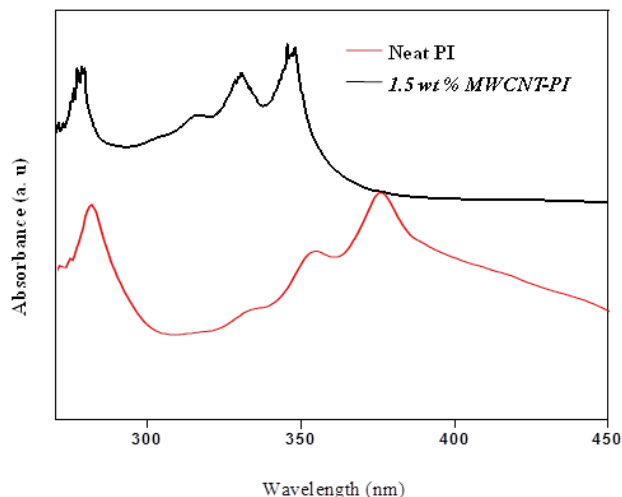


Figure 7. UV-Visible absorption spectra of neat PI and MWCNT-PI nanocomposites

The MWCNT incorporated PI nanocomposites (MWCNT-PI) displayed a band at 288 nm and another absorption band corresponding to the pyrene π - π^* transitions revealed the successful uniform dispersion of MWCNT into the PI matrix [34].

4.6.2 Photoluminescence spectra

The photoluminescence properties of neat PI and MWCNT-PI nanocomposites were investigated under the irradiation of UV-vis light with a wavelength of 365 nm as shown in Figure 8. The polymer emits blue fluorescence in THF solution with a major fluorescence emission at 360 and a minor emission at 405 nm for neat PI. It is evident that the emission peak originated from the pyrene structure present in the polyimide matrix [34, 48].

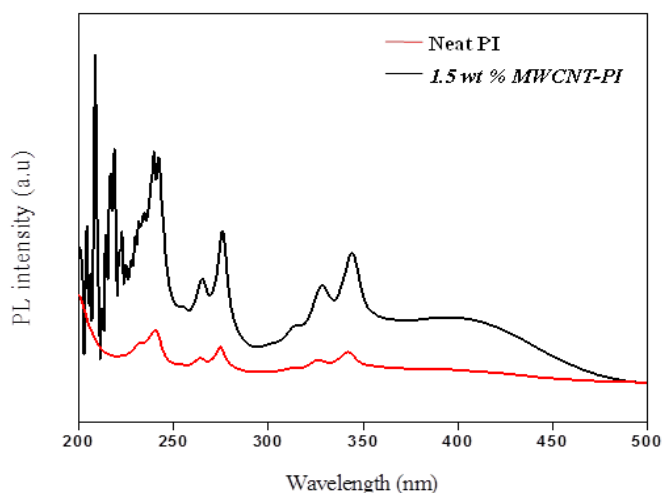


Figure 8. Photoluminescence patterns of neat PI and MWCNT-PI nanocomposites

No apparent changes were observed for the absorption of MWCNT incorporated PI nanocomposites (Figure 8). This study further confirms the uniform level dispersion of MWCNTs in the polyimide matrix. Thus, these polyimides could be attributed to the presence of rigid, highly fluorescent pyrene chromophore and confirmed their structural formation. Hence, such aromatic heterocyclic polymers can be used for light-emitting diode materials for high performance opto-electronic applications.

4.7 Morphological Properties

4.7.1. X-ray Diffraction Analysis

X-ray diffraction (XRD) patterns of the neat PI and MWCNT-PI nanocomposites are shown in Figure 9. The MWCNT incorporated PI nanocomposites show the characteristic diffraction peak corresponding to α -MWCNT [35]. Thus, this pattern of diffraction peaks confirmed the reinforcement of MWCNT in the polyimide matrices, which indicated the successful formation of nanocomposites.

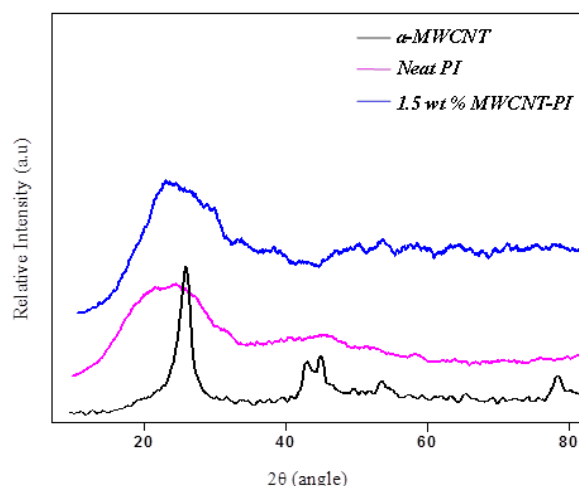


Figure 9. XRD patterns of neat PI and MWCNT-PI nanocomposites

4.7.2. SEM Analysis

The morphological properties of the neat polyimide system and MWCNT/PI nanocomposites were investigated by SEM studies. Figure 10a shows the smooth and homogeneous morphology of the neat PI matrix. Moreover, there was no distinguishable phase separation, and dark regions were observed without macroscopic phase separation, as seen in Figure 10a. It is evident that the homogeneous dispersion of the MWCNT (Figure 10b) arose from the miscibility of the acid functionalized MWCNT within the PI matrix, due to the strong interfacial interactions (covalent and hydrogen bonds) as well as the chemical compatibility between the PI matrix and the acid functionalized MWCNTs [35].

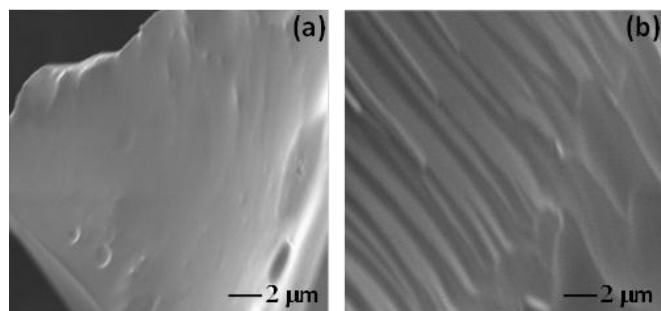


Figure 10. SEM images of (a) neat PI (b) 1.5 wt % MWCNT-PI nanocomposites

4.7.3. TEM Analysis

Figures 11a and b represent the TEM images of neat and MWCNT/PI nanocomposites. There is a smooth morphology as seen from Figure 11a. No deterioration and no confined domains in and around the region of the MWCNTs (Figure 11b), after incorporating into PI matrix was observed [37]. Thus, this dispersion is responsible for making MWCNT reinforced polymer nanocomposites, with excellent thermal, electrical and mechanical properties.

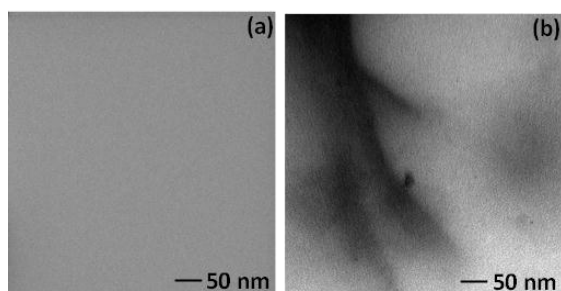


Figure 11. TEM images of (a) neat PI (b) 1.5 wt % MWCNT-PI nanocomposites

5. CONCLUSION

A novel polyimide containing pyridine core diamine and MWCNT reinforced PI nanocomposites have been structurally designed and developed using siloxane core dianhydride. The MWCNT acts as good nanofiller and it enhances the thermooxidative stability, glass transition temperature and dielectric constant of the nanocomposites. The data from the thermal studies indicate that the thermal stability of MWCNT-PI nanocomposites was better than that of neat PI. The T_g of the MWCNT/PI nanocomposites were also higher due to the combination of heterocyclic pyridine core, siloxane-imide, as well as the constraint effect of MWCNT. The resulted nanocomposites possess an increased dielectric constant values with increment in the loading level of MWCNT. The MWCNT/PI nanocomposites yielded higher char to about 15-30 % than that of the neat PI. The improved LOI (13 %) of the MWCNT/PI nanocomposites could be offered as flame retardant materials. The neat PI emits blue fluorescence arisen from the pyrene structure confirmed by

PL spectra. The uniform dispersion of MWCNTs into the PBZ was also confirmed by the diffraction pattern. The morphological studies evidence the compatibility, homogeneous successful incorporation of MWCNT of MWCNT into the matrix. Thus, these nanocomposites are expected to find high performance applications in the fields of aerospace, high temperature EMI shielding and microelectronics for better performances and high longevity.

ACKNOWLEDGEMENT

The authors acknowledge Dr. R. Jayavel, Director, Centre for Nanoscience and Nanotechnology, Anna University, Chennai, India for providing DSC and SEM analytical facility. The author also acknowledges Mr. K. Srinivasan and Mr. K. Rajakumar, for their vital support in photoluminescence analysis, Department of Chemistry, Anna University, Chennai, India and thanks IITM, Chennai, India for providing TEM facility.

REFERENCES

- [1] M. Hasegawa, K. Horie, "Photo physics, photochemistry and optical properties of polyimides," *Prog. Polym. Sci.*, vol. 26 (2), 2001, pp. 259-335.
- [2] N. Jain, S. K. Tripathi, M. Nasim, "Preparation and characterization of aminopropylsilatrane endcapped polyimide films," *Int. J. Polym. Mater.*, vol. 63 (4), 2013, pp. 178-184.
- [3] M. Enhessari, M. Shaterian, K. Ozaee, E. Karamali, "Synthesis and thermal properties of polyimide-BaZrO₃ novel nanocomposites," *Polym. Plast. Technol. Eng.*, vol. 51 (4), 2012, pp. 345-349.
- [4] X. L. Wang, Y. F. Li, C. L. Gong, T. Ma, F. C. Yang, "Synthesis and properties of new pyridine-bridged poly (ether-imide)s based on 4-(4-trifluoromethylphenyl)-2,6-bis[4-(4-aminophenoxy) phenyl] pyridine," *J. Fluor. Chem.*, vol. 129 (1), 2008, pp. 56-63.
- [5] C. P. Yang, S. H. Hsiao, K. L. Wu, "Organosoluble and light-colored fluorinated polyimides derived from 2,3-bis (4-amino-2-trifluoro methyl phenoxy) naphthalene and aromatic dianhydrides," *Polymer*, vol. 44 (23), 2003, pp. 7067-7078.
- [6] D. J. Liaw, B. Y. Liaw, C. W. Yu, "Synthesis and characterization of new organosoluble polyimides based on flexible diamine," *Polymer*, vol. 42 (12), 2001, pp. 5175-5179.
- [7] D. J. Liaw, B. Y. Liaw, "Synthesis and properties of new polyimides derived from 1, 1-bis [4-(4-aminophenoxy) phenyl] cyclododecane," *Polymer*, vol. 40 (11), 1999, pp. 3183-3189.

- [8] K. L. Wang, W. T. Liou, D. J. Liaw, W. T. Chen, "A novel fluorescent poly (pyridine-imide) acid chemo sensor," *Dyes Pigments*, vol. 78 (2), 2008, pp. 93–100.
- [9] Q. Y. Zhang, S. H. Li, W. M. Li, S. B. Zhang, "Synthesis and properties of novel organosoluble polyimides derived from 1,4-bis [4-(3,4-dicarboxylphenoxy)] triptycene dianhydride and various aromatic diamines," *Polymer*, vol. 48 (21), 2007, pp. 6246–6253.
- [10] M. Mukesh Kumar, S. Arun Kashinath, B. Susanta, P. Shashi, "Synthesis and properties of fluorinated polyimides, derived from novel 2,6-bis (30-trifluoromethyl-p-aminobiphenyl ether) pyridine and 2,5-bis (30-trifluoromethyl-p-aminobiphenyl ether) thiophene," *Macromol. Chem. Phys.*, vol. 203 (9), 2002, pp. 1238–1248.
- [11] C. L. Chung, S. H. Hsiao, "Novel organosoluble fluorinated polyimides derived from 1,6-bis (4-amino-2-trifluoromethyl phenoxy) naphthalene and aromatic dianhydrides," *Polymer*, vol. 49 (10), 2008, pp. 2476–2485.
- [12] B. Voit, "The potential of cycloaddition reactions in the synthesis of dendritic polymers," *New J. Chem*, vol. 31 (7), 2007, pp. 1139–51.
- [13] B. Bruchmann, "Dendritic polymers based on urethane chemistry-syntheses and applications," *Macromol Mater Eng*, vol. 292 (9), 2007, pp. 981–992.
- [14] C. R. Yates, W. Hayes, "Synthesis and applications of hyperbranched polymers," *Eur. Polym. J.*, vol. 40(7), 2004, pp. 1257–81.
- [15] M. Jikei, M. A. Kakimoto, "Dendritic aromatic polyamides and polyimides," *J. Polym. Sci. A Polym. Chem*, vol. 42 (6), 2004, pp. 1293–1309.
- [16] Y. Liao, J. Weber, C. F. J. Faul, "Fluorescent microporous polyimides based on perylene and triazine for highly CO₂-selective carbon materials," *Macromolecules*, vol. 48 (7), 2015, pp. 2064–2073.
- [17] Y. Luo, B. Li, L. Liang, B. Tan, "Synthesis of cost-effective porous polyimides and their gas storage properties," *Chem. Commun*, vol. 47 (27), 2011, pp. 7704.
- [18] R. Hobzova, J. Peter, P. Sysel, "Hyperbranched polymers," *Chem. Listy*, vol. 102 (10), 2008, pp. 906–913.
- [19] J. Fang, H. Kita, K. I. Okamoto, "Gas permeation properties of hyperbranched polyimide membranes," *J. Membr. Sci.*, vol. 182 (1–2), 2001, pp. 245–56.
- [20] T. Suzuki, Y. Yamada, Y. Tsujita, "Gas transport properties of 6FDA-TAPOB hyperbranched polyimide membrane," *Polymer*, vol. 45 (21), 2004, pp. 7167–71.
- [21] X. W. Jiang, Y. Z. Bin, M. Matsuo, "Electrical and mechanical properties of polyimide-carbon nanotubes composites fabricated by in situ polymerization," *Polymer*, vol. 46 (18), 2005, pp. 7418–7424.
- [22] E. Kymakis, I. Alexandou, G. A. J. Amaratunga, "Single-walled carbon-polymer composites: electrical, optical and structural investigation," *Syn. Met.*, vol. 127 (1–3), 2002, pp. 59–62.
- [23] H. Zeng, C. Gao, Y. Wang, "In situ polymerization approach to multi-walled carbon nanotubes reinforced nylon 1010 composites: Mechanical properties and crystallization behaviour," *Polymer*, vol. 47 (1), 2006, pp. 113–122.
- [24] J. J. Ge, D. Zhang, Q. Li, H. Hou, M. J. Graham, L. Dai, F. W. Harris, S. Z. D. Cheng, "Multi-walled carbon nanotubes with chemically grafted polyetherimides," *J. Am. Chem. Soc.*, vol. 127 (28), 2005, pp. 9984–9985.
- [25] L. W. Qu, Y. Lin, D. E. Hill, B. Zhou, W. Wang, X. F. Sun, A. Kitaygorodskiy, M. Suarez, J. W. Connell, L. F. Allard, Y. P. Sun, "Polyimide functionalized carbon nanotubes: synthesis and dispersion in nanocomposites," *Macromolecules*, vol. 37 (16), 2004, pp. 6055–6060.
- [26] S. M. Yuen, C. M. C. C. Ma, C. L. Chiang, "Morphology and properties of aminosilane grafted MWCNT/polyimide nanocomposites," *J. Nanomater*, vol. 2008, 2008, pp. 1–15.
- [27] K. D. Ausman, R. Piner, O. Lourie, R. S. Ruoff, M. Korobov, "Organic solvent dispersions of SWCNTs: toward solution of pristine nanotubes," *J. Phys. Chem. B*, vol. 104 (38), 2000, pp. 8911–8915.
- [28] T. Liu, Y. Tong, W. D. Zhang, "Preparation and characterization of carbon nanotube/polyetherimide," *Comp. Sci. Tech*, vol. 67 (3–4), 2007, pp. 406–412.
- [29] A. Chandramohan, S. Nagendiran, M. Alagar, "Synthesis and characterization of polyhedral oligomeric silsesquioxane-siloxane-modified polyimide hybrid nanocomposite," *J. Compos. Mater*, vol. 46 (7), 2012, pp. 773–781.
- [30] Z. Q. Tao, S. Y. Yang, J. S. Chen, L. Fan, "Synthesis and characterization of imide ring and siloxane-containing cycloaliphatic epoxy resins," *Eur. Polym. J.*, vol. 43 (4), 2007, pp. 1470–1479.

- [31] L. A. S. A. De Prado, I. L. Torriani, I. V. P. Yoshida, "Poly (n-alkylsilsequioxane)s: Synthesis, characterization, and modification with poly(dimethylsiloxane)," *J. Polym. Sci. B Polym. Chem*, vol. 48 (5), 2010, pp. 1220–1229.
- [32] H. T. Li, M. S. Lin, H. R. Chuang, M. W. Wang, "Siloxane and imide modified epoxy resin cured with siloxane containing dianhydride," *J. Polym. Res*, vol. 12 (5), 2005, pp. 385–391.
- [33] K. C. Chen, H. T. Li, S. C. Huang, W. B. Chen, K. W. Sun, F. C. Chang, "Synthesis and performance enhancement of novel polybenzoxazines with low surface free energy," *Polym. Int*, vol. 60 (7), 2011, pp. 1089–1096.
- [34] S. G. Gunasekaran, M. Dharmendirakumar, "Siloxane core-modified organo soluble novel polyimide/multi-walled carbon nanotube nanocomposites," *Polym Plast. Technol. Eng*, vol. 53 (9), 2014, pp. 903–916.
- [35] R. Padhma Priya, S. G. Gunasekaran, M. Dharmendirakumar, "Phthalide cardo chain extended siloxane core skeletal modified polyimide/multi-walled carbon nanotube nanocomposites," *J. Nanosci Nanotechnol*, vol. 15 (9), 2015, pp. 6739–6746.
- [36] S. G. Gunasekaran, K. Rajakumar, M. Alagar, M. Dharmendirakumar, "Design and development of mesoporous silica reinforced skeletal modified triaryl pyridine core based polybenzoxazine (SBA-15/PBZ) nanocomposites," *Int. J. Plast. Technol*, vol. 19 (2), 2015, pp. 309–332.
- [37] S. G. Gunasekaran, K. Rajakumar, M. Dharmendirakumar, "Organo modified multi-walled carbon nanotube reinforced pyridine core polybenzoxazine (MWCNT/PBZ) nanocomposites," *Int. J. Nanosci*, vol. 14(5 & 6), 2015, pp. 1550021-1550033.
- [38] S. G. Gunasekaran, S. Devaraju, M. Alagar, M. Dharmendirakumar, "Studies on synthesis and characterization of multi-walled carbon nanotube-reinforced polyimide nanocomposites based on a siloxane-modified anhydride," *High Perform. Polym*, vol. 26 (1), 2014, pp. 43–51.
- [39] X. L. Wang, Y. F. Li, S. J. Zhang, T. Ma, Y. Shao, X. Zhao, "Synthesis and characterization of novel polyimides derived from pyridine-bridged aromatic dianhydride and various diamines," *Eur. Polym. J*, Vol. 42 (6), 2006, pp. 1229–1239.
- [40] K. L. Wang, W. T. Liou, D. J. Liaw, S. T. Huang, "High glass transition and thermal stability of new pyridine-containing polyimides: effect of protonation on fluorescence," *Polymer*, vol. 49 (6), 2008, pp. 1538–1546.
- [41] R. Hariharan, S. Bhuvana, M. Anitha Malbi, M. Sarojadevi, "Synthesis and characterization of polyimides containing pyridine moiety," *J. Appl. Polym Sci*, Vol. 93 (4), 2004, pp. 1846–1853.
- [42] M. A. Shahram, M. M. Rezvaneh, N. Majid, "Synthesis and characterization of heat resistant, pyridine-based polyimides with preformed ether and ester groups," *Eur. Polym. J*, vol. 41 (5), 2005, pp. 1024–1029.
- [43] B. Tamami, H. Yeganeh, "Preparation and properties of novel polyimides derived from 4-aryl- 2, 6 bis (4-amino phenyl) pyridine," *J. Polym. Sci. A Polym. Chem*, vol. 39 (21), 2001, pp. 3826–3831.
- [44] A. Hirsch, "Functionalization of single-walled carbon nanotubes," *Angew Chem. Int. Ed*, vol. 41 (11), 2002, pp. 1853–1859.
- [45] S. Devaraju, M. R. Vengatesan, A. Ashok Kumar, M. Alagar, "Polybenzoxazine-silica (PBZ-SiO₂) hybrid nanocomposites through in situ sol-gel method," *J. Sol-Gel Sci. Technol*, vol. 60 (1), 2011, pp. 33–40.
- [46] T. Takeichi, T. Agag, R. Zeidam, "Preparation and properties of polybenzoxazine- poly (imide-siloxane) Alloys: In situ ring-opening polymerization of benzoxazine in the presence of soluble poly (imidesiloxane)s," *J. Polym. Sci. A Polym. Chem*, Vol. 39 (15), 2001, pp. 2633–2641.
- [47] Y. L. Liu, Y. C. Chiu, C. S. Wu, "Preparation of silicon-phosphorous containing epoxy resins from the fusion process to bring a synergistic effect on improving the resins: thermal stability and flame retardancy," *J. Appl. Polym. Sci*, vol. 87 (3), 2003, pp. 404–411.
- [48] D. J. Liaw, K. L. Wang, F. C. Chang. Novel organosoluble poly (pyridine-imide) with pendent pyrene group: synthesis, thermal, optical, electrochemical, electrochromic, and protonation characterization. *Macromolecules*, vol. 40 (10), 2007, 3568–3574.
- [49] B. Tamami, H. Yeganeh, "Preparation and properties of novel polyimides derived from 4-aryl-2, 6 bis (4-amino phenyl) pyridine. *J. Polym. Sci. A Polym. Chem*, vol. 39 (21), 2001, 3826–3831.
- [50] Y. Watanabe, Y. Shibasaki, S. Ando, M. Ueda, "Synthesis and characterization of polyimides with low dielectric constants from aromatic dianhydrides and aromatic diamine containing phenylene ether unit," *Polymer*, vol. 46 (16), 2005, pp. 5903–5908.

- [51] B. S. Kim, S. H. Bae, Y. H. Park, J. H. Kim, "Preparation and characterization of polyimide/carbon-nanotube composites," *Macromol. Res*, vol. 15 (4), 2007, pp. 357-362.
- [52] Z. Ounaies, C. Park, K. E. Wise, E. J. Siochi, J. S. Harrison, "Electrical properties of single wall carbon nanotube reinforced polyimide composites," *Compos. Sci. Technol*, vol. 63 (11), 2003, pp. 1637-1646.
- [53] S. C. Gupta, A. Shivhare, D. Singh and S. Gupta. Melamine Polyimide Composite Fire Resistant Intumescent Coatings. *Def. Sci. J*, vol. 63 (6), 2013, pp. 442-446.